Available online at www.sciencedirect.com
SCIENCE DIRECT
Polymer 47 (2006) 56–66
polymer
www.elsevier.com/locate/polymer

Copolymerization behavior of Cp_2ZrCl_2/MAO and [$(CO)_5W{=}C(Me)OZrCp_2Cl$]/MAO: a comparative study on ethylene/1-pentene copolymers

Nyambeni Luruli [a,*], Lars-Christian Heinz [b], Valérie Grumel [a], Robert Brüll [b], Harald Pasch [b], Helgard G. Raubenheimer [a]

[a] *Department of Chemistry and Polymer Science, University of Stellenbosch, Private Bag X1, 7602 Matieland, South Africa*
[b] *Deutsches Kunststoff-Institut (German Institute for Polymers), Schloßgartenstr. 6, 64289 Darmstadt, Germany*

Received 31 July 2005; received in revised form 6 November 2005; accepted 10 November 2005
Available online 28 November 2005

Abstract

Ethylene/1-pentene copolymers were synthesized using Cp_2ZrCl_2(**1**)/MAO and [$(CO)_5W{=}C(Me)OZr(Cp)_2Cl$](**2**)/MAO catalyst systems. The copolymers were characterized by SEC, DSC, FTIR and ^{13}C NMR spectroscopy. The copolymers synthesized with [$(CO)_5W{=}C(Me)OZr(Cp)_2Cl$](**2**)/MAO had higher average molecular weights and broader polydispersities compared to those produced with Cp_2ZrCl_2(**1**)/MAO. The chemical heterogeneity was investigated by SEC-FTIR and fractionation techniques. All copolymers showed a higher incorporation of the 1-pentene in the low molecular weight fraction as revealed by SEC-FTIR. Crystallization analysis fractionation (CRYSTAF) showed a broad chemical composition distribution (CCD) for all the copolymers synthesized with these two catalyst systems. Selected copolymers were also analyzed using an automated preparative molecular weight fractionation.

Keywords: Ethylene/1-pentene copolymers; Short chain branching distribution (SCBD); Automated preparative molecular weight fractionation (PMWF)

1. Introduction

Metallocene/MAO catalyst systems were discovered about 25 years ago by Kaminsky and coworkers [1,2]. The catalyst Cp_2ZrCl_2(**1**)/MAO was among the first metallocene catalyst systems to be investigated with regard to polymerization behavior in the early 1980's [3,4]. Since then, metallocene/MAO and single site catalysts in general have developed into more complex systems [5]. The modification of the metallocene structure brought improvements in catalyst activities and comonomer incorporation (in the case of copolymers) and thus affording many possibilities to improve polymer properties.

The final properties of a polymer are, on a molecular level, influenced by the molecular weight distribution, the average chemical composition and the chemical heterogeneity. The latter classifies the distribution of the comonomer units, microstructural parameters and endgroups along and perpendicular to the molecular weight axis. These parameters strongly influence the final polymer properties and current research focuses on tailoring these by catalyst or process modification.

It is generally accepted that metallocene catalysts produce polyolefins with narrow molecular weight distributions and studies have proven this for many examples including the catalyst system, **1**/MAO [3,6–8]. Although it is also claimed that the copolymers produced with metallocenes have a homogeneous incorporation of the comonomer, little experimental evidence can be found to support this [9–11].

Our group has been working on, among others, the synthesis of Fischer-type carbene complexes for hydroformylation and polymerization of α-olefins utilizing metallocene catalysts [12–15]. Metalloxycarbenes [16,17] are well known, however, we do not know of a study involving their use as potential olefin polymerization catalysts except by us [12]. The first catalyst system we reported prior to metalloxycarbenes was an alkoxy $Cp_2Zr(Cl)OMe$/MAO, which is virtually inactive towards 1-pentene oligomerization [15]. On the other hand, when the chlorine ligand in Cp_2ZrCl_2 (**1**) is substituted with a Fischer-type ligand [$(CO)_5W{=}C(Me)OLi$] to form [$(CO)_5W{=}C(Me)OZr(Cp)_2Cl$](**2**)/MAO catalyst system, activities substantially higher than those of $Cp_2Zr(Cl)OMe$/MAO are achieved for the oligomerization of 1-pentene [15]. The zirconoxycarbene complex, (**2**), has potential as a catalyst

* Corresponding author. Tel.: +27 21 808 3165; fax: +27 21 808 4967.
E-mail address: luruli@sun.ac.za (N. Luruli).

0032-3861/$ - see front matter © 2005 Elsevier Ltd. All rights reserved.
doi:10.1016/j.polymer.2005.11.042

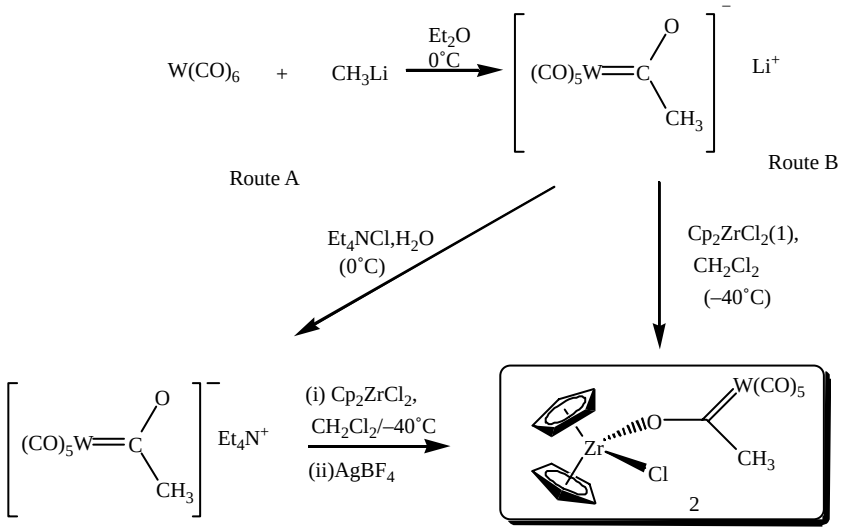

Scheme 1. Reaction scheme showing the synthesis reaction of $[(CO)_5W{=}C(Me)OZr(Cp)_2Cl]$ (**2**).

precursor since about four variables can be manipulated in order to fine-tune its polymerization behavior and consequently influence the polymer properties. Understanding the polymerization behavior of this catalyst precursor is, therefore, important for further studies involving both catalyst design and polymerizations.

As an extension to the study of the copolymerization of ethylene with 1-pentene utilizing **2**/MAO reported earlier [12], in this paper we compare the copolymerization behavior of **2** and Cp_2ZrCl_2 (**1**)/MAO in terms of the properties of ethylene/1-pentene copolymers produced. Particular emphasis was given to the chemical heterogeneity, investigated by hyphenated SEC-FTIR and fractionation techniques.

2. Experimental

2.1. Materials

All materials (tungstenhexacarbonyl, methyllithium, Et_4NCl and $AgBF_4$) used for the preparation of complex **2** were obtained from SIGMA-Aldrich and used as received. Ethylene, polymerization grade, was purchased from Fedgas and used without further purification. 1-Pentene was obtained from SASOL, South Africa. It was dried by refluxing over $LiAlH_4$ and then distilled under nitrogen. Methylaluminoxane (10% w/v solution in toluene) and Cp_2ZrCl_2 were purchased from SIGMA-Aldrich and used as received. Toluene (SIGMA-Aldrich) was dried by refluxing over sodium/benzophenone and then distilled under an inert gas atmosphere.

2.2. The synthesis of $[(CO)_5W{=}C(Me)OZr(Cp)_2Cl]$ (2)

The catalyst precursor $[(CO)_5W{=}C(Me)OZr(Cp)_2Cl]$ (**2**)] was prepared according to Scheme 1 [12,18,19]. Tungsten hexacarbonyl was reacted with methyllithium in diethylether at 0 °C to yield the corresponding anionic Fischer-type carbene complex. Excess starting material, $W(CO)_6$, was removed from the dried lithium salt by washing with pentane. Higher yields of the metalloxycarbene complexes were obtained by first converting the carbene salt to a tetraethylammonium (route A). Addition of $AgBF_4$ to a mixture of carbene salt $[(CO)_5W_1{=}C(R)O]NEt_4$ and $Cp_2Zr_2Cl_2$ (**1**) in dichloromethane

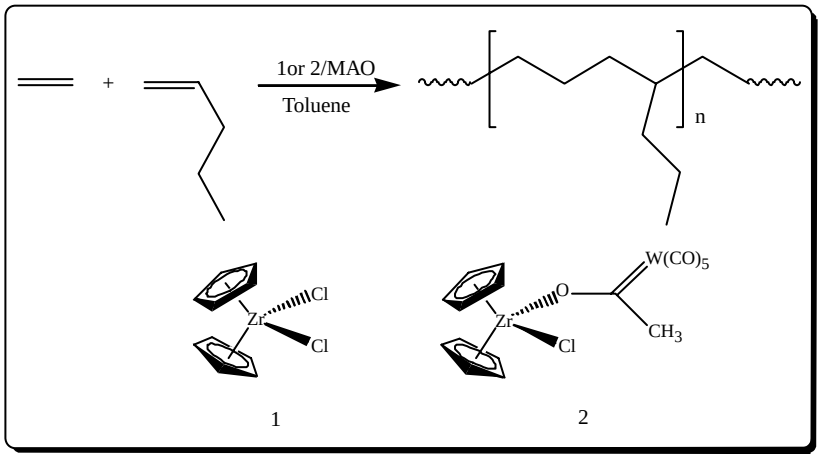

Scheme 2. Polymerization reaction scheme for ethylene/1-pentene copolymers.

Table 1
The summary of NMR, GPC, DSC and CRYSTAF results for ethylene/1-pentene copolymers

Sample code	Catalyst no.	1-Pentene in the feed (mol%)	1-Pentene in the copolymer (mol%)	CRYSTAF sol. fraction (%)	$T_{c\ CRYSTAF}$ (°C)	$T_{c\ DSC}$ (°C)	$T_{m\ DSC}$ (°C)	M_n (g/mol)	M_w (g/mol)	PDI	Activity (kg mol^{-1} h^{-1})
ZrA	1	0	0	0	87.7	119.5	132.4	41,700	119,000	2.8	133.3
Zr1	1	29.1	9.0	31.7	78.7	106.2	114.7	7000	26,000	3.8	503.0
Zr2	1	60.6	14.9	58.2	54.7	95.3	102.2	6300	15,700	2.5	67.9
Zr3	1	29.1	4.5	5.6	73.2	104.4	116.8	14,200	39,400	2.8	64.2
Zr4	1	16.1	7.0	15.6	78.3	108.6	118.1	13,000	46,500	3.6	84.8
Zr5	1	33.9	8.6	22.7	76.8	96.0	105.2	17,400	40,000	2.3	84.2
Zr6	1	47.3	16.1	60.1	Non	92.8	100.9	8500	20,000	2.4	109.1
Zr7	1	55.2	5.2	8.6	76.4	104.5	116.8	29,600	87,000	2.9	46.5
WA	2	0	0	0	87.5	116.9	134.1	44,900	225,900	5.0	266.7
W1	2	9.3	0.2	0	86.2	114.8	133.8	235,600	772,900	3.3	176.4
W3	2	29.1	2.3	7.4	85.3	113.8	130.0	47,500	245,100	5.2	283.0
W4	2	45.1	2.0	8.3	83.9	110.6	129.9	18,700	156,200	8.4	357.6
W5	2	55.2	3.9	10	82.3	111.0	124.6	18,300	218,400	11.9	262.4
W6	2	60.6	7.0	35.9	80.3	107.0	119.4	2500	126,600	50.5	285.5
W7	2	43.5	2.0	10.7	84.3	114.1	127.3	26,500	185,500	7.0	254.5
W8	2	50.6	5.3	12.3	81.8	110.4	122.9	81,700	317,300	3.9	309.1
W9	2	64.2	3.9	14.6	82.7	112.0	125.0	20,000	321,100	16.0	280.6

encouraged the removal of chloride from the metallocene centre, and formation of the Zr–O bond. By-products of this reaction, AgCl and $[Et_4N]BF_4$, were removed by filtration.

2.3. General polymerization procedure

All reactions were carried out under an inert gas atmosphere using standard Schlenk techniques. Polymerization reactions were performed in a 350 ml stainless steel batch reactor (Parr) fitted with an inlet valve and pressure gauge. A glass liner was used in the reactor. Generally, the reagents were introduced into the reactor in the following order: catalyst precursor, MAO and the comonomer (Scheme 2). For each catalyst, the moles of ca. 5.5×10^{-3} mmol in 30 ml of toluene per run were used. Amounts of 1-pentene in the feed were varied from 10–60 mol% (Table 1) relative to the total number of moles used. Thereafter, the reactor was saturated with ethylene gas, kept constant at about 5 g for each run. The catalyst/MAO ratio was kept at 1:1000 throughout. All the reactions were carried out at room temperature for 3 h. The polymers were isolated by precipitation in acidic methanol, washed thoroughly with methanol and subsequently dried in vacuum at 65 °C for 10 h.

2.4. Characterization of the polymers

The comonomer incorporation was determined using ^{13}C NMR spectroscopy, using 1,2,4-trichlorobenzene/C_6D_6 (9:1) as solvent and measuring at 100 °C on a Varian VXR-300 (75 MHz) NMR spectrometer.

Molecular weights of the polymers were determined using a PL 220 chromatograph from Polymer Laboratories fitted with five Waters Styragel columns (HT 2–6), at a flow rate of 1 ml/min in 1,2,4-trichlorobenzene at 140 °C, relative to narrowly distributed polystyrene standards. The eluent was stabilized with Irganox 1010 to prevent degradation.

Thermal analyses were conducted under nitrogen on a Mettler Toledo DSC 822, at a heating and cooling rate of 10 °C/min, using about 6 mg of the samples. In order to erase the thermal history, two heating cycles and one cooling cycle were run. The maxima and minima of the second heating and cooling curves were analyzed and recorded as melting and crystallization temperatures, respectively.

A CRYSTAF apparatus, model 200 from PolymerChar S.A (Valencia, Spain), was used for fractionation. Samples (20 mg) were dissolved in 30 ml of distilled 1,2,4-trichlorobenzene at 160 °C. After dissolution, the temperature was decreased at a rate of 0.1 °C/min.

Infrared spectra were acquired using a Nicolet Nexus spectrometer in ATR-Mode and Omnic 5.2 software for interpretation. Typically 60 scans at a resolution of 2 cm^{-1} were accumulated for each sample.

An LC-transform Model 300 from LabConnections, coupled to a Waters 150C chromatograph (columns HT 2–6) was used for the SEC-FTIR analyses. The stage temperature was 160 °C, the temperature of the nozzle 125 °C and the transfer line was operated at 150 °C. The rotating speed of the Germanium disc was 10 °/min.

The preparative molecular weight fractionations (PMWF) were carried out with a fully automated preparative TREF equipment (PREP mc2®)[1] using solvent/non-solvent gradient elution. The copolymer (500 mg) was dissolved in a combination of xylene (solvent) and diethyleneglycolmonobutylether (non-solvent) at 130 °C according to temperature program (Scheme 3). The temperature was then lowered to 110 °C at 30 °C/min. Finally, the temperature was raised to 120 °C at a rate of 20 °C/min for elution. This cycle was repeated for each fraction over a solvent gradient. The fractions

[1] PREP mc2® is a commercial preparative TREF equipment manufactured by PolymerChar, Valancia, Spain.

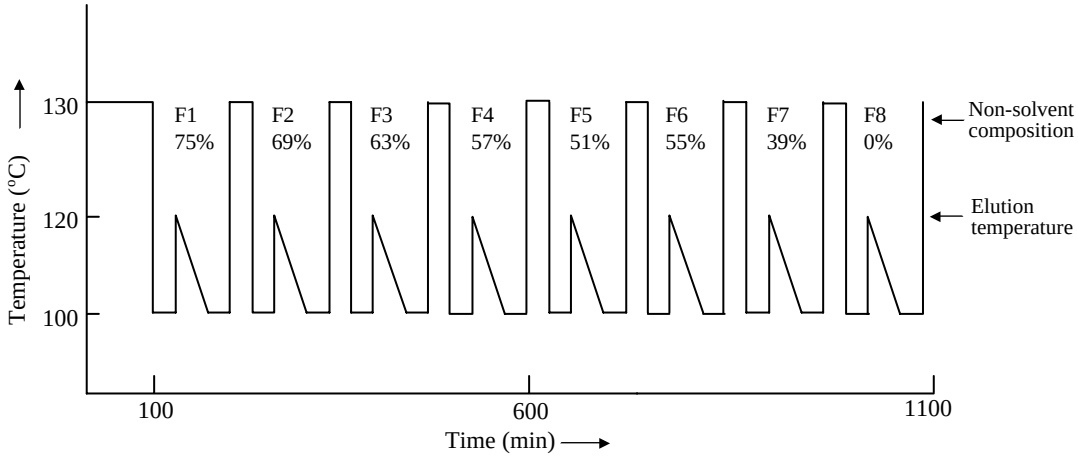

Scheme 3. Temperature program for preparative molecular weight fractionation (PMWF).

were collected at 6% intervals of solvent/non-solvent composition gradient starting from 75% of non-solvent. The fractionated polymers were precipitated in 100 ml of acetone while stirring and thoroughly washed with methanol. Finally, the polymer was dried over night in an oven at 50 °C. The fractions were then analyzed using SEC, DSC, FTIR, CRYSTAF and NMR. Fractions containing residual diethyleneglycolmonobutylether (DEGMBE) were crystallized from xylene and dried before performing further analysis.

3. Results and discussion

The catalytic and molecular characterization data are summarized in Table 1. As can be seen, the activities for **2**/MAO were higher than those of **1**/MAO. Generally, ethylene/1-pentene copolymers synthesized with **1**/MAO had weight average molecular weights (M_w) below 100,000 g/mol and relatively narrow polydispersities (Table 1). Fig. 1 shows representative molecular weight distribution curves of these copolymers. Narrow molecular weight distributions prove that **1**/MAO exhibits metallocene behavior characteristics as expected [3,20,21]. On the other hand, high weight average molecular weight (M_w) above 100,000 g/mol and broad (sometimes bimodal) distributions were observed for copolymers synthesized with **2**/MAO (Fig. 2). As we observed previously, the copolymers produced with **2**/MAO are characterized by high polydispersities. The average molecular weights of ethylene/1-pentene copolymers produced by both catalyst systems decreased with increasing comonomer content in the copolymers. High comonomer concentration promotes chain transfer reactions to the comonomer resulting in the reduction of the average molecular weight. This phenomenon has been previously observed on various catalyst systems involving α-olefins copolymerizations [20–23].

The molecular weight of polyolefins produced via coordination polymerization is controlled by steric factors around the active site. Usually, an increase in the steric factors around the active site or coordination center brought about by a bulky ligand retards β-hydride elimination, making chain transfer to the monomer more difficult and resulting in the formation of

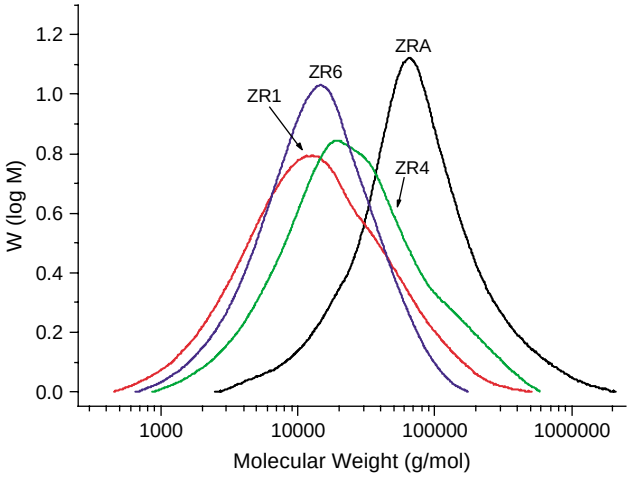

Fig. 1. Molecular weight distribution curves of ethylene/1-pentene copolymers synthesized with Cp_2ZrCl_2(**1**)/MAO.

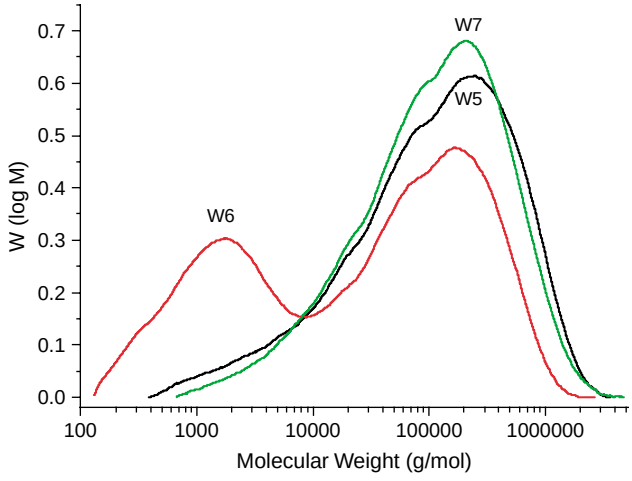

Fig. 2. Molecular weight distribution curves of ethylene/1-pentene copolymers synthesized with **2**/MAO.

high molecular weight polymers or copolymers [20,21,24]. It is known that ionic pair formation is extremely important in determining catalytic activity. Due to the relatively long Zr–O bond (2.034 Å) in the complex $[(CO)_5W{=}C(Me)OZr(Cp)_2Cl]$ (**2**)/MAO (crystal structure of such complex to be published elsewhere), we assume that this bond would be heterolytically cleaved in the formation of the active cationic catalyst just as one Cl would be replaced by CH_3 from MAO. This would result in the formation of a Cp_2ZrMe^+ species (as in the case of **1**/MAO) and adduct formation between $(CO)_5W{=}C(Me)O^-$ and MAO. This ionic pair interaction could be responsible for both the high molecular weights of the ethylene/1-pentene copolymers, as a result of hindered β-H elimination reactions, as well as the higher catalytic activity exhibited by **2**/MAO compared to **1**/MAO. However, other types of ion pair interactions could also be responsible for the generation of different types of active species producing bimodal and multimodal copolymers.

Broad MWDs are consistent with the preliminary results we published earlier for ethylene/1-pentene copolymers synthesized with **2**/MAO [12]. The amount of comonomer incorporation was determined using ^{13}C NMR [25]. The copolymers synthesized with **1**/MAO showed higher comonomer incorporation when comparable feed stream compositions were used. Previously, we restricted the comonomer incorporation to low amounts. With the aim of fully understanding the comonomer incorporation behavior of **2**, the amount of 1-pentene was not limited in this study. The comonomer incorporation for copolymers produced with **2**/MAO could not exceed 7% even after increasing the concentration of 1-pentene in the feed stream to more than 60% but decreased instead (for example W 9). During polymerization chain propagation competes with chain termination reactions. Comonomer and cocatalyst, among others, promote chain transfer which leads to chain termination [26–30]. While steric hindrance in **2**/MAO helps to increase the molecular weight by suppressing chain termination reactions, increasing comonomer concentration leads to a point where chain transfer to the monomer overcomes chain propagation, ultimately leading to low average molecular weight and finally, low comonomer incorporation [20,24,31,32]. Although the chemical structure of $(CO)_5W{=}C(Me)OZr(Cp)_2Cl$ (**2**), would fit metallocene definition [11,33,34] the molecular weight distributions of polymers or copolymers produced with this catalyst system at ambient temperature strengthen the conclusion we made before that these catalyst systems are not metallocene catalyst systems but instead behave like Ziegler–Natta catalysts [12].

Fig. 3 shows the melting and crystallization temperatures as a function of comonomer content for copolymers synthesized with **2**/MAO. Although the melting and crystallization temperatures decrease with increasing comonomer content, the deviation from a linear relationship can well be observed. Most of the copolymers synthesized with **1**/MAO showed multiple (two or three) melting and crystallisation transitions as measured by DSC while those produced with **2**/MAO only showed single transition during both heating and cooling.

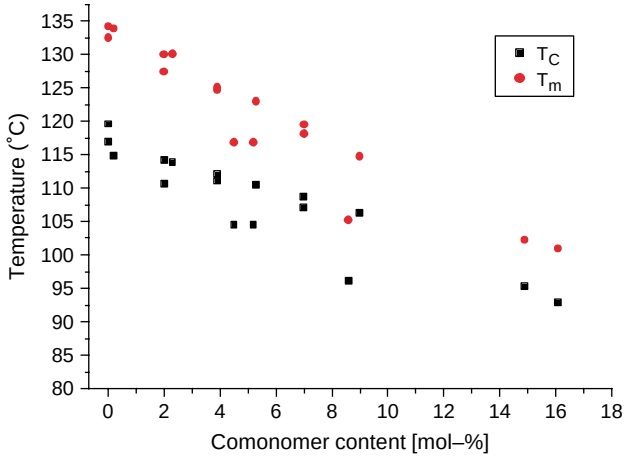

Fig. 3. Melting (T_m) and crystallization (T_c) temperatures vs. comonomer content of copolymers produced with **1** and **2**/MAO.

The melting and crystallization temperatures reported in Table 1 are values corresponding to the highly crystalline materials only. These multiple DSC transitions indicate that the copolymers have a broad CCD. Alternatively, this can result from a combination of melting and crystallization processes. This can be proven by applying different heating rates as shown in Fig. 4. For example, three distinct melting peaks were

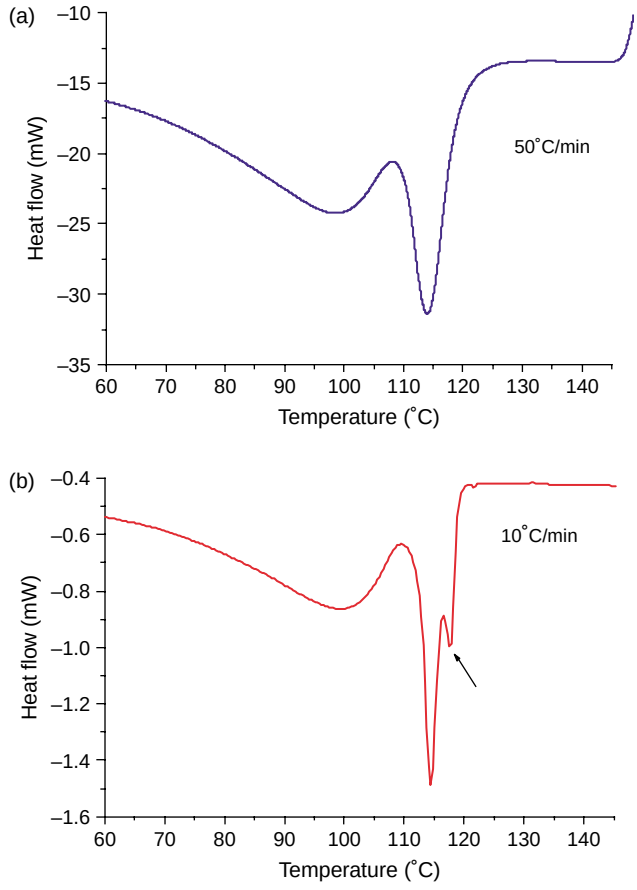

Fig. 4. DSC heating curves of sample ZR1 measured using heating rate of 50 °C/min (a) and 10 °C/min (b).

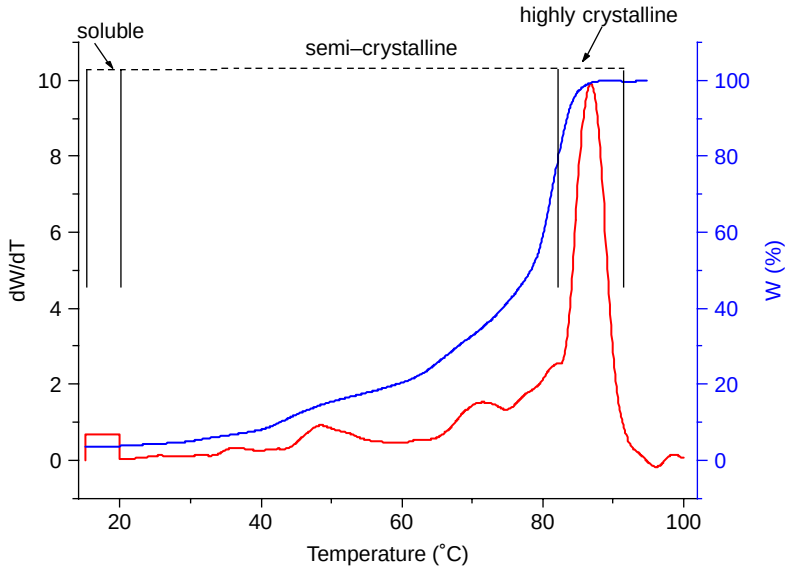

Fig. 5. Typical CRYSTAF profile for semi-crystalline polymers.

observed for sample ZR1 (Fig. 4) during slow heating. However, when fast heating rates were applied, a recrystallization peak (indicated by an arrow) disappeared owing to the fact that the chains were not given enough time to recrystallize. Nevertheless, two melting peaks remained even after applying fast heating scans. Multiple DSC transitions for metallocene catalyzed polymers have previously been associated with broader CCD of the copolymers [35]. Other studies have shown that the active sites in metallocenes catalyst systems in general, are not all homogeneous resulting in the formation of polymers with multiple thermal transitions or broad CCD or high degree of chemical heterogeneity [26,36,37].

The chemical heterogeneity describes the distribution of comonomers, endgroups and microstructural parameters along and perpendicular to the molecular weight axis. It can be analyzed by fractionation according to molecular weight

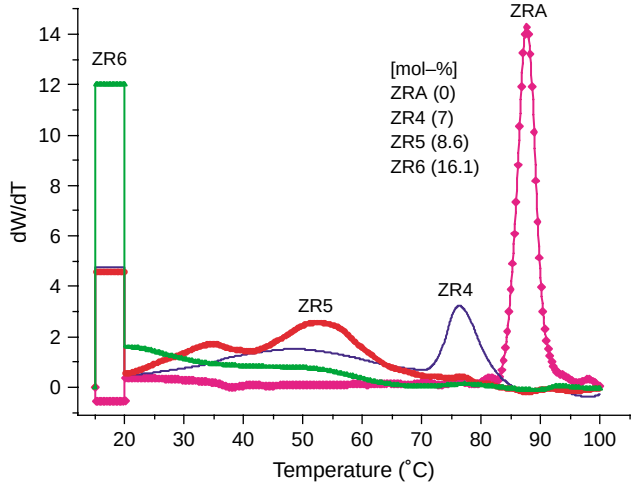

Fig. 6. CRYSTAF profiles of ethylene/1-pentene copolymers synthesized with **1**/MAO.

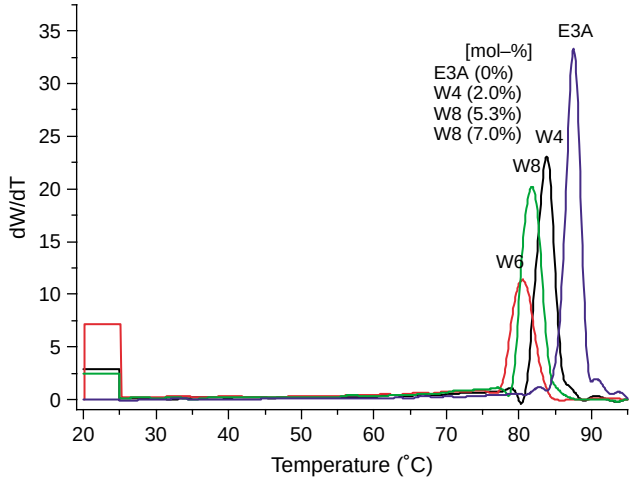

Fig. 7. CRYSTAF profiles of ethylene/1-pentene copolymers synthesized with **2**/MAO.

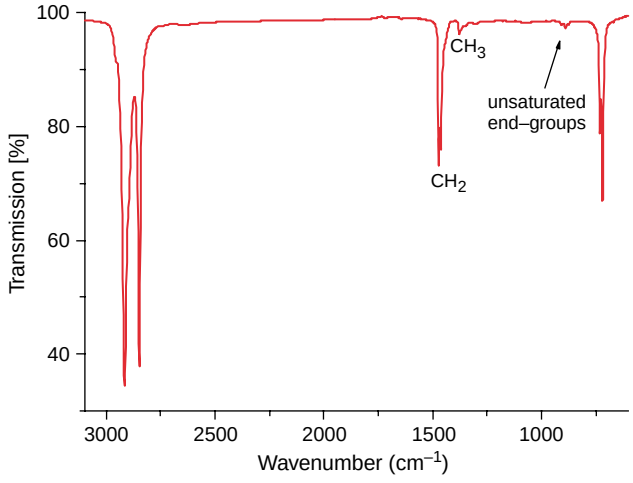

Fig. 8. Typical FTIR spectrum of ethylene/1-pentene copolymer.

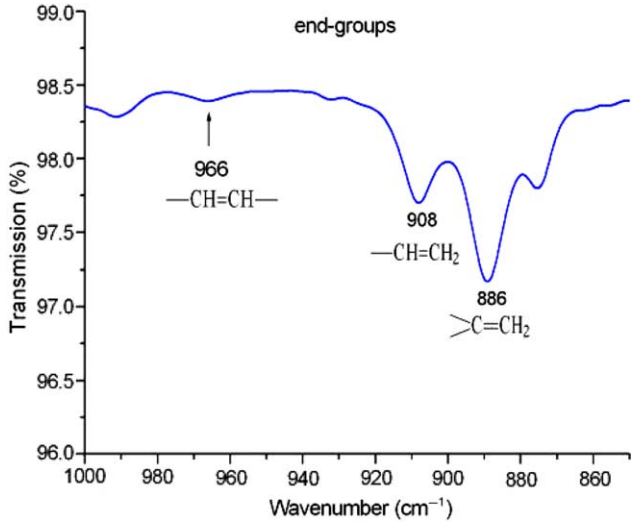

Fig. 9. Unsaturated end-group region of the FTIR spectrum of ethylene/1-pentene copolymers.

coupled with spectroscopic detection and by compositional fractionation, respectively.

CRYSTAF fractionates semi-crystalline materials according to their crystallizability from solution. Typically, a sample is dissolved at a temperature above crystallization. After complete dissolution, the polymer is allowed to crystallize by reducing the temperature at a slow rate. Aliquots of the polymer solution are filtered and the concentration of the polymer in solution analyzed by an infrared detector. Details of this technique have been published earlier [38–40]. A typical CRYSTAF profile (Fig. 5) consists of a cumulative curve and its first derivative. The first derivative is generally associated with the CCD of a polymer and will be referred to as CRYSTAF profile or curve in this study. Figs. 6 and 7 show the overlay of the CRYSTAF profiles of ethylene/1-pentene copolymers synthesized with **1** and **2**/MAO, respectively. Generally, the crystallization profiles for both series slightly broaden relative to the homopolymers with increasing comonomer content and simultaneously the amount of soluble fraction increases. These trends are in agreement with

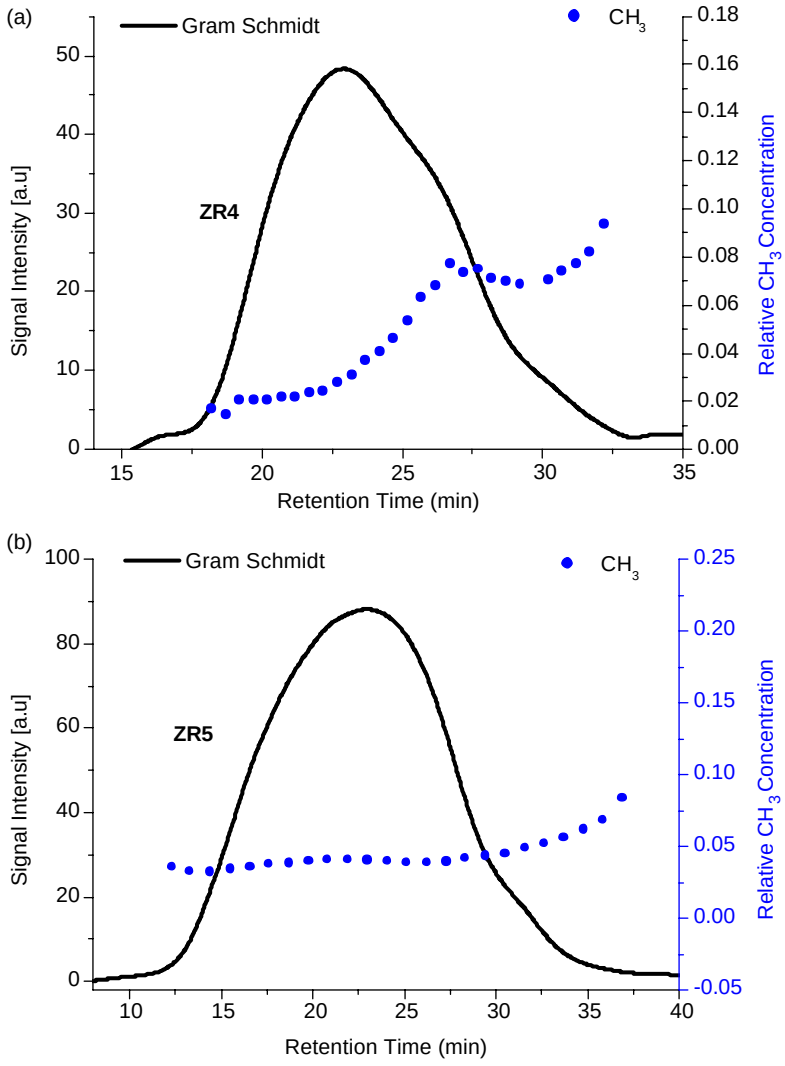

Fig. 10. SEC-FTIR results of ethylene 1-pentene copolymers synthesized by **1**/MAO.

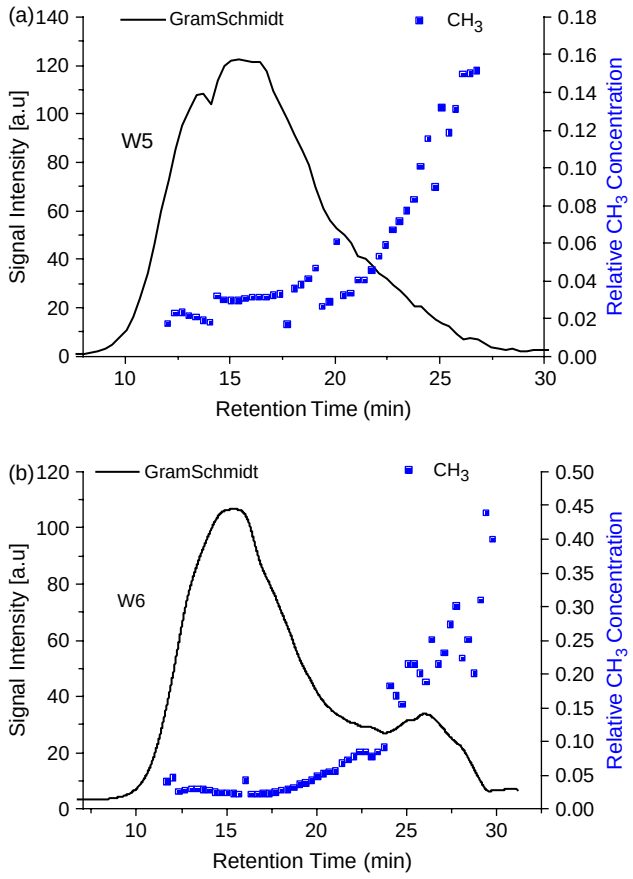

Fig. 11. SEC-FTIR results of ethylene 1-pentene copolymers synthesized by **2**/MAO.

CRYSTAF results which have been obtained for copolymers synthesized with *rac*-Et(Ind)$_2$ZrCl$_2$/MAO [40,41]. For both series, the peak crystallization temperatures decrease with increase in comonomer content as already observed on DSC analysis. The crystallization peak finally disappeared for copolymers with high comonomer content e.g. ZR6. Comparing the CRYSTAF profiles of the copolymers with similar amounts or percentages of comonomer from both series, it can be observed that copolymers synthesized with **1**/MAO show crystallization below the main peak, whereas the same behavior is not observed for copolymers produced with **2**/MAO. Taking these facts into account it can be concluded that **2**/MAO produces chemically more homogeneous copolymers than **1**/MAO. In order to study the distribution of 1-pentene along the molecular weight axis, the copolymers were analyzed by SEC-FTIR via LC-Transform.

In the LC-Transform approach, the polymer in the eluent is deposited on a rotating Germanium disc via nubilization of eluent. The trace on the polymer sample carrier, Germanium disc, is then analyzed off-line using FTIR. From the spectra taken around the disc, the software re-constructs the Gram-Schmidt plot which gives concentration profiles that resemble refractive index signals (or molecular weight distribution curves) of high temperature SEC. Chemigrams are then generated from the data to profile the intensity of a particular wavenumber along the molecular weight axis [42,43].

The compositional analysis of an ethylene copolymers by FTIR is well established [44–47]. The typical IR spectrum of ethylene/1-pentene copolymer is shown in Fig. 8. The absorption bands at 1379 and 1460 cm^{-1} correspond to the methyl and methylene groups, respectively. Fig. 9 depicts the enlargement of the unsaturated endgroup region in the FTIR spectrum. The absorption band at 887 cm^{-1} corresponds to vinylidene ($R_2C{=}CH_2$), 908 cm^{-1} to vinyl ($RCH{=}CH_2$) and 966 cm^{-1} to *trans*-vinylene (RCH=CHR). The SEC-FTIR analysis from both series is shown in Figs. 10 and 11. All copolymers investigated, regardless of the catalyst used, showed an increase in the 1-pentene concentration (relative CH_3) towards the low molecular weight fraction. However, copolymers synthesized with **2**/MAO (Fig. 11) showed a sharper increase compared to those synthesized with **1**/MAO. The heterogeneous comonomer distribution on copolymers obtained by both of these catalyst systems, can be explained by

Table 2
The summary of molecular weight fractionation data

Frac no.	$T_{c\ DSC}$ (°C)	$T_{m\ DSC}$ (°C)	M_n (g/mol)	M_w (g/mol)	PDI	Yield (mg)	Yield (%)
(a) Sample ZR4							
1	107.8	116.0	8500	18,300	2.2	118.3	23.7
2	109.5	117.2	13,300	23,400	1.8	60.1	12.0
3	110.0	118.2	19,500	32,700	1.7	50.0	10.0
4	110.3	119.0	26,100	45,000	1.8	45.2	9.0
5	110.5	120.5	50,200	77,000	1.5	38.9	7.8
6	109.7	120.3	50,900	118,000	2.3	40.7	8.1
7	108.7	119.7	80,600	240,000	3.0	70.3	14.1
(b) Sample W5							
1	113.0	122.2	10,400	74,200	7.1	128.8	30.9
2	113.1	123.3	35,600	135,000	3.8	55.8	13.4
3	113.7	123.8	50,500	135,000	2.7	42.0	10.1
4	113.3	123.5	68,600	139,000	2.0	41.9	10.1
5	111.2	124.8	102,000	230,000	2.2	34.6	8.3
6	111.7	124.7	120,000	213,000	1.8	45.2	10.8
7	109.5	124.8	242,000	383,000	1.6	69.2	16.6

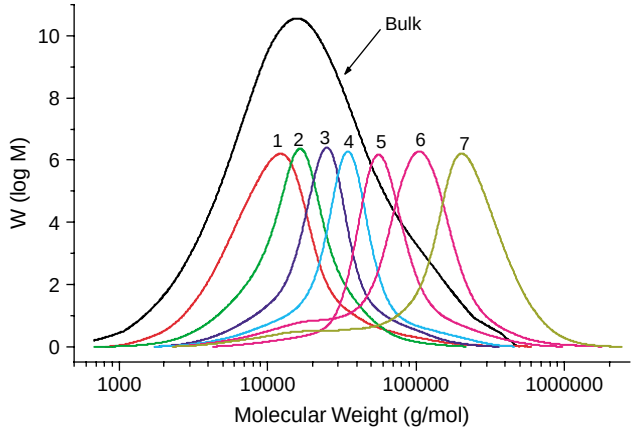

Fig. 12. Molecular weight distribution profiles of the bulk sample and PMWF fractions of sample ZR4 synthesized with **1**/MAO.

the lack of a bridging ligand which could restrict the rotation or movements of the Cp-ligands during polymerization. Although we do not know of a study involving SEC-FTIR analysis of polyolefin copolymers synthesized with Cp_2ZrCl_2/MAO, non-ansa metallocene catalyst systems have previously shown a heterogeneous comonomer distribution [9,48]. On the other hand ethylene/α-olefin copolymers, synthesized using the bridged catalyst system, *rac*Et[Ind]$_2$ZrCl$_2$/MAO, which were investigated by us using SEC-FTIR [49], showed a more homogeneous comonomer distribution than observed for **1** or **2**/MAO

Profiling the unsaturated endgroups using the bands at 887, 908 and 966 cm^{-1} remained unsuccessful, as the thickness of the deposit on the Germanium disc was not sufficient. To overcome this problem selected samples (ZR4 and W5) from each catalyst were fractionated by preparative molecular weight fractionation using a combination of solvent /non-solvent. This technique for fractionating semicrystalline polymers according to molecular weight been developed in the 1970's [50]. However, automated preparative molecular weight fractionation (PMWF) was briefly introduced recently by Monrabal [39]. In a step-gradient of xylene (solvent) and

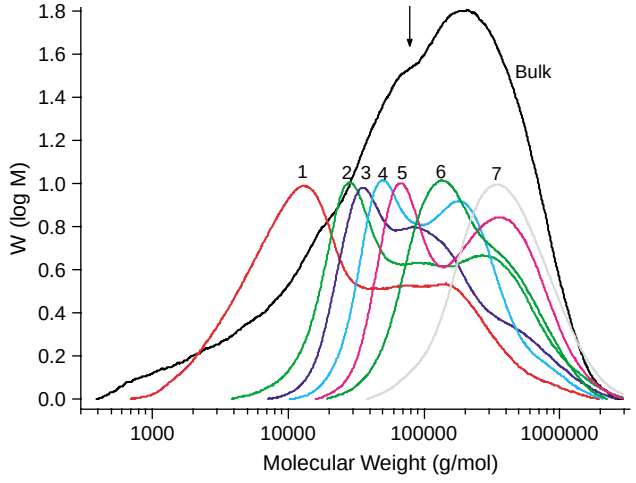

Fig. 13. Molecular weight distribution profiles of the bulk samples and PMWF fractions of sample W5 synthesized with **2**/MAO.

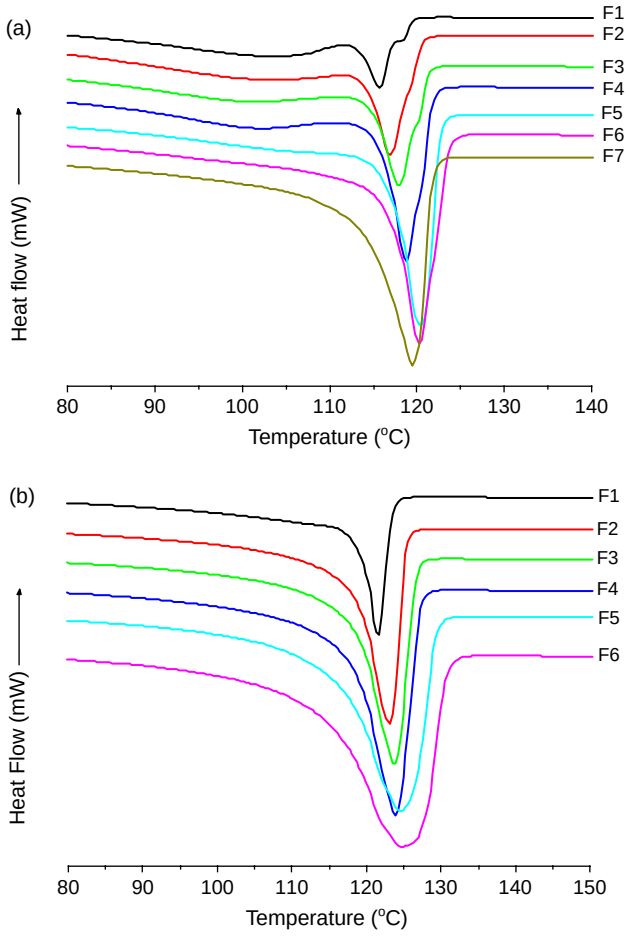

Fig. 14. DSC curves (melting region) of (a) ZR4 and (b) W5 molecular weight fractions of copolymers synthesized with **1** and **2**/MAO, respectively.

DEGMBE (non-solvent) we were able to fractionate the samples according to molecular weight. Each fraction was then analyzed by SEC, DSC, FTIR, and ^{1}H NMR spectroscopy with regard to thermal properties, molecular weight distribution content and unsaturation. The characterization data from SEC and DSC are summarized in Table 2. The overlay of

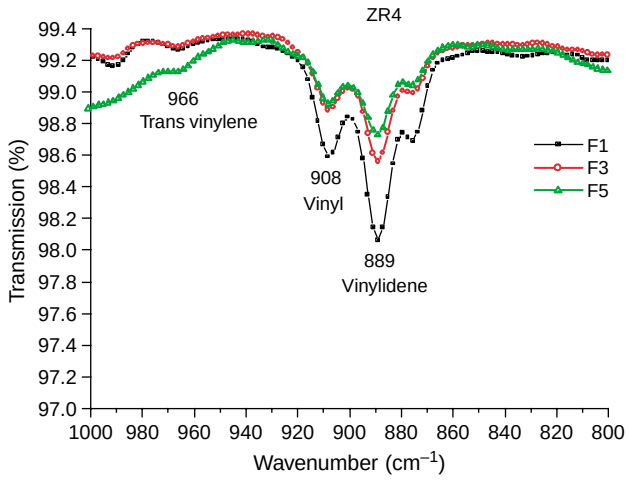

Fig. 15. Enlargement of the unsaturated end-group region in the FTIR spectrum of (a) ZR4 fractions.

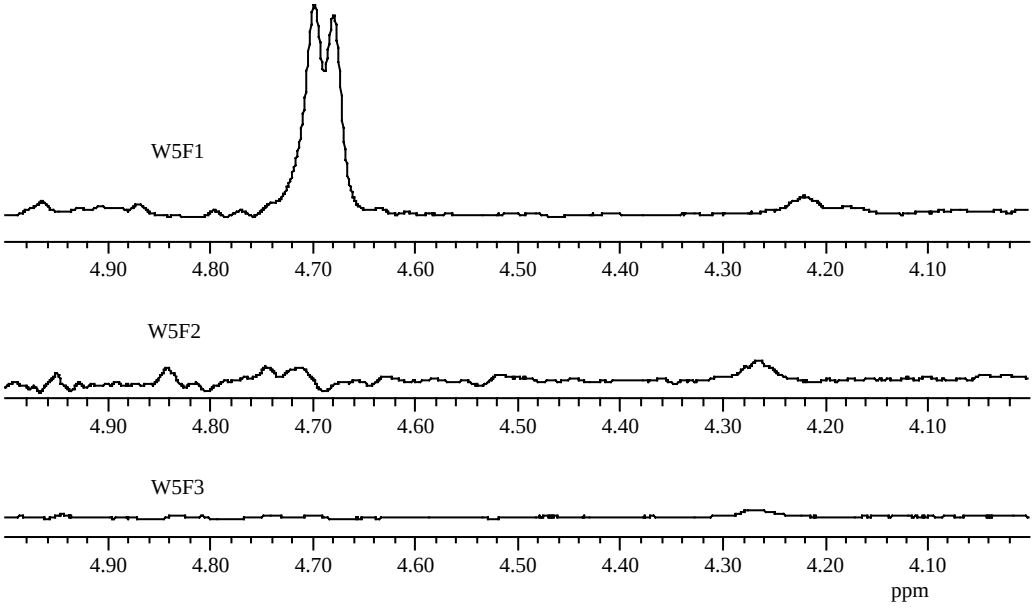

Fig. 16. ^{1}H NMR spectrum showing vinylidene end-group region of W5 fractions.

the molecular weight distribution curves for the fractions and the bulk of samples ZR4 and W5, shown in Figs. 12 and 13, indicate that the separation takes place mainly according to molecular weight. It must be noted that it is impossible to separate exclusively according to molecular weight without the influence of chemical composition or vice versa [51].

It is clear that the fractions of sample ZR4 show narrow polydispersities over a broad range of molecular weight while the low molar mass fractions of W5 have broad and bimodal molecular weight distributions (Figs. 12 and 13). It is interesting to note that the bimodality of W5 fractions (Fig. 13) occurred around the same molecular weight range where the bimodal distribution of the bulk sample is found.

As expected from the results of the SEC-FTIR analysis, the melting and crystallization temperatures of the fractions as measured by DSC increased with their average molecular weight for both the samples (ZR4 and W5) (Fig. 14(a) and (b)). It is interesting to note that the low molar mass fractions of ZR4 have multiple melting peaks indicating that broadening of the CCD occurs towards low molecular weight region.

The relative concentrations of vinyl and *trans*-vinylene endgroups were analyzed from IR spectroscopy. Fig. 15 shows the endgroup region of FTIR spectra of the selected fractions for sample ZR4. As seen, the endgroups (vinyl and *trans*-vinylene) concentration is higher in the low molecular weight fractions. The FTIR analysis for the endgroups of W5 also followed the same trend. As the vibration of the vinylidene groups overlaps with the CH_3-rocking vibration of the comonomer, the relative concentration of the vinylidene endgroups was analyzed from the ^{1}H NMR using the resonance between 4.6 and 4.8 ppm. It is difficult to see the endgroups on high molecular weight fractions. To avoid the molecular weight effect, we only analyzed the vinylidene content of the first three fractions of each samples, i.e., with relatively low molecular weight. Fig. 16, which is the overlay of ^{1}H NMR spectrum of the first three fractions of W5, clearly indicates that vinylidene concentration is high in the first fraction while the other two contain virtually no trace. Similarly, the vinylidene concentration for ZR4 was high in the low molar mass fractions as analyzed by ^{1}H NMR spectroscopy.

The chemical composition distribution of the copolymers produced by these two catalyst systems perpendicular to their molar mass axis is summarized by a schematic representation shown in Fig. 17. The scheme shows that heterogeneous comonomer distribution occurs in both cases with high comonomer concentration towards low molecular weight. However, **2**/MAO copolymers show a sharper increase in the comonomer content on copolymers chains with low molecular weight.

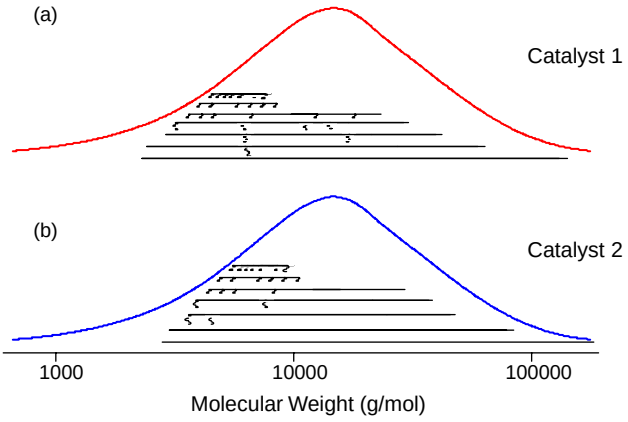

Fig. 17. Schematic representation of comonomer distribution along the molecular weight axis.

4. Conclusion

Copolymers produced with the catalyst systems **2**/MAO show remarkable differences compared with materials synthesized with Cp_2ZrCl_2/MAO. These differences become obvious, when fractionation techniques such as CRYSTAF, PMMF and SEC-FTIR are used. The results obtained clearly indicate that **2** behaves rather like a Ziegler–Natta catalyst system. It is also evident that the carbene ligand plays a role—at least sterically during polymerization as evidenced by higher molecular weight copolymers obtained with **2**/MAO than copolymers produced with Cp_2ZrCl_2/MAO.

Acknowledgements

N.L. thanks the DAAD for financial support towards this project. The financial support of this work by the National Research Foundation (NRF) and South African Department of Labor (DoL) is gratefully acknowledged. Authors would like to thank Mr C. Brinkmann and Mrs C. Hock for SEC and FTIR measurements, respectively.

References

[1] Sinn H, Kaminsky W, Vollmer HJ. Angew Chem, Int Ed 1980;19:390.
[2] Sinn H, Kaminsky W. Adv Organomet Chem 1980;18:99.
[3] Kaminsky W. J Polym Sci, Part A: Polym Chem 2004;42:3911.
[4] Löfgren B, Kokko E, Seppälä J. Adv Polym Sci 2004;169:1.
[5] Alt HG, Koppl A. Chem Rev 2000;100:1205.
[6] Cho HS, Chung JS, Han JH, Ko YG, Lee WY. J Appl Polym Sci 1998;70:1707.
[7] Byun D, Kim SY. Macromolecules 2000;33:1921.
[8] Seppälä JV, Koivumäki J, Liu X. J Polym Sci, Part A: Polym Chem 1993;31:3447.
[9] Soga K, Uozumi T, Arai T, Nakamura S. Macromol Rapid Commun 1995;16:379.
[10] Xu XR, Xu JT, Feng LX, Chen W. Acta Polym Sin 1998;4:502.
[11] Starck P, Lehmus P, Seppälä JV. Polym Eng Sci 1999;39:1444.
[12] Luruli N, Grumel V, Brüll R, Du Toit A, Pasch H, van Reenen AJ, et al. J Polym Sci, Part A: Polym Chem 2004;42:5121.
[13] Brüll R, Luruli N, Pasch H, Raubenheimer HG, Sadiku ER, Sanderson RD, et al. e-Polymer 2003;061.
[14] Brüll R, Pasch H, Raubenheimer HG, Sanderson RD, van Reenen AJ, Wahner UM. Macromol Chem Phys 2001;202:1281.
[15] Brüll R, Kgosane D, Nevelling A, Pasch H, Raubenheimer HG, Sanderson RD, et al. Macromol Symp 2001;165:11.
[16] Barluenga J, Santamaría J, Tomás M. Chem Rev 2004;104:2259.
[17] Barluenga J, Fañanás F. Tetrahedron 2000;56:4597.
[18] Neveling A. MSc Thesis, University of Stellenbosch, Stellenbosch, South Africa; 1999.
[19] Nel J. MSc Thesis, University of Stellenbosch, Stellenbosch, South Africa; 2002.
[20] Ko YS, Woo SI. J Polym Sci, Part A: Polym Chem 2003;41:2171.
[21] Czaja K, Białek M, Utrata A. J Polym Sci, Part A: Polym Chem 2004;42:2512.
[22] Naga N, Imanishi Y. Macromol Chem Phys 2002;203:771.
[23] Czaja K, Białek M. Polymer 2001;42:2289.
[24] Naga N, Imanishi Y. J Polym Sci, Part A: Polym Chem 2003;41:441.
[25] Randall JC. Polym Charact ESR NMR Symp 1980;6:93.
[26] Heiland K, Kaminsky W. Makromol Chem Phys 1992;193:601.
[27] Quijada R, Dupont J, Miranda MSL, Scipioni RB, Galland GB. Macromol Chem Phys 1995;196:3991.
[28] Schneider MJ, Suhm J, Mulhaupt R, Prosenc MH, Brintzinger HH. Macromolecules 1997;30:3164.
[29] Quijada R, Galland GB, Mauler RS. Macromol Chem Phys 1996;197:3091.
[30] Byun DJ, Shin DK, Kim SY. Polym Bull 1999;42:301.
[31] Camurati I, Cavicchi B, Dall'Occo T, Piemontesi F. Macromol Chem Phys 2001;202:701.
[32] Lehmas P, Harkki O, Leino R, Luttikhedde HJG, Nasman JH, Seppala JV. Macromol Chem Phys 1998;199:1965.
[33] Alt HG, Köppl A. Chem Rev 2000;100:1205.
[34] Resconi L, Cavallo L, Fait A, Piemontesi F. Chem Rev 2000;100:1253.
[35] Xu X, Xu T, Feng L, Chen W. J Appl Polym Sci 2000;77:1709.
[36] Quijada R, Galland GB, Freitas LL, da Jornada JAH, Mauler RS, Miranda MSL. Polym Bull 1995;35:299.
[37] Mirabella FM, Bafna A. J Polym Sci, Part A: Polym Chem 2002;40:1637.
[38] Monrabal B, Blanco J, Nieto J, Soares JBP. J Polym Sci, Part A: Polym Chem 1999;37:89.
[39] Monrabal B. In: Mayers RA, editor. Temperature rising elution fractionation and crystallization analysis fractionation. Encyclopedia of analytical chemistry, vol. 14; 2000, 2000. p. 1–20.
[40] Sarzotti DM, Soares JBP, Penlidis A. J Polym Sci, Part B: Polym Phys 2002;40:2595.
[41] Sarzotti DM, Soares JBP, Simon LC, Britto LJD. Polymer 2004;45:4787.
[42] Faldi A, Soares JBP. Polymer 2001;42:3057.
[43] Verdumen-Noël L, Baldo L, Bremmers S. Polymer 2001;42:5523.
[44] Neves CJ, Monteiro E, Habert AC. J Appl Polym Sci 1993;50:817.
[45] Blitz JP, McFaddin DC. J Appl Polym Sci 1994;51:13.
[46] Hongjun C, Xiaolie L, Dezhu M, Jianmin W, Hongsheng T. J Appl Polym Sci 1999;71:93.
[47] Tackx P, Bremmers S. Polym Matter Sci Eng 1998;78:50.
[48] Kakugo M, Miyatake T, Mizunuma K. Macromolecules 1991;24:1469.
[49] Graef SM, Brüll R, Pasch H, Wahner UM. e-Polymers 2003;005.
[50] Bergström C, Avela E. J Appl Polym Sci 1979;23:163.
[51] Francuskiewicz F. Polymer fractionation. Berlin: Springer-Verlab; 1994 [chapter 12, p. 177].